Sex Does Not Influence Visual Outcomes After Blast-Mediated Traumatic Brain Injury but IL-1 Pathway Mutations Confer Partial Rescue

Lucy P. Evans,[1,2] Nickolas Boehme,[3] Shu Wu,[1] Elliot L. Burghardt,[2,4] Abhigna Akurathi,[3] Brittany P. Todd,[1,2] Elizabeth A. Newell,[1] Polly J. Ferguson,[1] Vinit B. Mahajan,[5,6] Laura M. Dutca,[3,7] Matthew M. Harper,[3,7] and Alexander G. Bassuk[1]

[1]Department of Pediatrics, University of Iowa, Iowa City, Iowa, United States
[2]Medical Scientist Training Program, University of Iowa, Iowa City, Iowa, United States
[3]Iowa City VA Health Care System Center for the Prevention and Treatment of Visual Loss, Iowa City, Iowa, United States
[4]Department of Biostatistics, University of Iowa, Iowa City, Iowa, United States
[5]Omics Laboratory, Byers Eye Institute, Department of Ophthalmology, Stanford University School of Medicine, Palo Alto, California, United States
[6]Veterans Affairs Palo Alto Health Care System, Palo Alto, California, United States
[7]Department of Ophthalmology and Visual Sciences, University of Iowa, Iowa City, Iowa, United States

PURPOSE. In a mouse model of blast-mediated traumatic brain injury (bTBI), interleukin-1 (IL-1)-pathway components were tested as potential therapeutic targets for bTBI-mediated retinal ganglion cell (RGC) dysfunction. Sex was also evaluated as a variable for RGC outcomes post-bTBI.

METHODS. Male and female mice with null mutations in genes encoding IL-1α, IL-1β, or IL-1RI were compared to C57BL/6J wild-type (WT) mice after exposure to three 20-psi blast waves given at an interblast interval of 1 hour or to mice receiving sham injury. To determine if genetic blockade of IL-1α, IL-1β, or IL-1RI could prevent damage to RGCs, the function and structure of these cells were evaluated by pattern electroretinogram and optical coherence tomography, respectively, 5 weeks following blast or sham exposure. RGC survival was also quantitatively assessed via immunohistochemical staining of BRN3A at the completion of the study.

RESULTS. Our results showed that male and female WT mice had a similar response to blast-induced retinal injury. Generally, constitutive deletion of IL-1α, IL-1β, or IL-1RI did not provide full protection from the effects of bTBI on visual outcomes; however, injured WT mice had significantly worse visual outcomes compared to the injured genetic knockout mice.

CONCLUSIONS. Sex does not affect RGC outcomes after bTBI. The genetic studies suggest that deletion of these IL-1 pathway components confers some protection, but global deletion from birth did not result in a complete rescue.

Keywords: blast, IL-1, retina, sex, visual function, TBI

Traumatic brain injury (TBI) is a complex injury that simultaneously damages multiple tissue types and can present both acutely or chronically following injury. TBI survivors suffer from physical and emotional sequelae, with permanent cognitive and sensory deficits.[1,2] Damage to the central nervous system (CNS) is often accompanied by visual disturbances, which are among the most common physical symptoms following a TBI.[3–6]

Blast-mediated TBI (bTBI) is a pervasive problem for military personnel, as over 400,000 U.S. service members have had at least one TBI within the last 20 years.[7] These effects have immediate consequences during active duty, as well as lingering chronic pathologies. After a bTBI, the link between cranial and ocular trauma is particularly strong,[8] causing long-term visual dysfunction, including light sensitivity, retinopathy, optic neuropathy, dysfunctional optic motility, disorders of refraction and accommodation, and visual field loss.[8–11]

In the brain, TBI activates signaling cascades that can elicit robust neuroinflammation and trigger progressive neuronal dysfunction, neuronal death, and tissue destruction.[12] TBI-induced neuroinflammatory signals include the interleukin-1 (IL-1) cytokine family, with IL-1α and IL-1β being the major pathway components that are rapidly upregulated in the TBI brain.[13,14] Both IL-1α and IL-1β signal through a common receptor, IL-1RI, and can contribute to CNS repair or secondary injury. Nevertheless, overwhelming evidence indicates that, after a TBI, neuronal damage is worsened by uncontrolled IL-1 signaling.[13,15]

Investigative Ophthalmology & Visual Science

The CNS, including the retina, is normally an immuno-privileged site that is sheltered from damaging systemic inflammatory responses.[16] Upon injury, resident surveillance cells (such as microglia and macroglia) are activated, resulting in a neuroinflammatory response that can lead to permanent tissue damage. Additionally, disruption of the blood–brain and blood–retina barrier can allow peripheral immune cells to invade and contribute further to this inflammatory response.[17] The increase in retinal inflammation after bTBI is documented in animal studies; nevertheless, how inflammation causes retinal pathogenesis is not well defined.[18–20]

In murine bTBI models, many groups (including ours) have found long-term deficits and cell death; most studies have focused particularly on the dysfunction and loss of retinal ganglion cell (RGCs).[18–24] RGC damage can permanently impair vision, resulting in major quality-of-life consequences; yet, the mechanisms responsible for bTBI-induced RGC dysfunction are not well understood. In recent experiments, the IL-1 pathway was pharmacologically blocked after bTBI to test whether acutely modulating this inflammatory IL-1 signaling might prevent subsequent neuronal deficits.[19] When the IL-1RI antagonist anakinra was used to block the acute inflammatory responses after bTBI, microglia and Müller glia activation was reduced. Additionally, anakinra reduced retinal neuroinflammation, which preserved optic nerve integrity, RGC function, and RGC layer thickness.[19] Still, this pharmacologic intervention did not provide complete protection, leaving unanswered questions concerning the efficacy of anakinra, the particular IL-1 molecules driving the visual pathology, and how to more effectively target the neuroinflammation that drives retinal damage after bTBI.

Hormonal differences between males and females might be expected to cause sex-specific responses to bTBI; however, there is currently no consensus as to whether sex acts as a biological variable in CNS injury pathogenesis.[25] The studies described here found that sex did not have a significant effect on the visual outcomes analyzed: survival of RGCs, RGC complex layer thickness, and RGC function. To determine whether deleting IL-1 pathway components protected the retina from bTBI-induced damage, visual outcomes were compared in wild-type (WT) versus mice with null mutations in genes encoding IL-1α, IL-1β, or IL-1RI. The complete deletion of IL-1 pathway components enabled this complementary study to parallel and compare the acute pharmacologic blockade of IL-1RI that was recently reported.[19]

MATERIALS AND METHODS

Animals

All animal studies were conducted in accordance with the ARVO Statement for the Use of Animals in Ophthalmic and Vision Research and were approved by the University of Iowa and Iowa City VA Health Care System Institutional Animal Care and Use Committee. IL-1α-, IL-1β-, or IL-1RI-deficient male and female mice (IL-1$\alpha^{-/-}$, IL-1$\beta^{-/-}$, and IL-1RI$^{-/-}$) backcrossed on a C57BL/6J genetic background were used; generation of these mice was previously described.[26,27] WT C57BL/6J male and female mice were purchased from The Jackson Laboratory (Bar Harbor, ME, USA) as controls. A total of 288 mice were used for this study, all 2 to 4 months of age (Supplementary Table S1).

Mice were housed under a 12-hour, light/dark cycle with ad libitum access to food and water.

Blast Injury Induction

An enclosed blast chamber was used, one half of which was pressurized, as previously described.[21] A plastic Mylar membrane (Mylar A, 0.00142 gauge; Country Plastics, Ames, IA, USA) was placed over a 13-cm opening separating the sides of the chamber. The unpressurized side of the tank contained a padded polyvinyl chloride (PVC) protective restraint in which an anesthetized mouse was placed. Compressed air was pumped into the pressurized side of the chamber until the membrane ruptured at 20 ± 0.2 psi (mean $\pm$ SEM, 137.8 ± 1.3 kPa), creating a blast wave with a duration of 10 to 15 ms. As many veterans are repeatedly exposed to blast forces, we administered three injuries to each mouse to mimic human injuries.[28–31] Mice were oriented within the chamber with the left side of the head positioned toward the blast wave (direct exposure) and the right side facing away from the direction of the blast wave (indirect exposure); they were then exposed to three blast injuries, each 1 hour apart. The mouse's body was shielded via the PVC restraint to limit blast wave pressure exposure primarily to the head; the head was allowed to move freely and was not in a fixed position. All analysis was conducted on the left (ipsilateral) side that was directly exposed to the blast wave, as we could not discount potential interaction between the contralateral eye and the padded holder or potential confounding, rebounding blast waves from the surface of the animal holder. Mice were anesthetized with a combination of ketamine (Ketalar, 30 mg/kg, intraperitoneally [IP]; Pfizer, Tadworth, UK) and xylazine (AnaSed Injection, 5 mg/kg, IP; Akorn, Inc., Lake Forest, IL, USA) before each blast or sham blast. They were then placed on a heating pad immediately following the blast injury to prevent hypothermia and to facilitate recovery from general anesthesia. Xylazine anesthesia was reversed with yohimbine chloride (1 mg/kg, IP; Diamondback Drugs, Scottsdale, AZ, USA) to aid in recovery from anesthesia. Control mice underwent an identical process in all respects except that they did not receive a blast exposure when placed in the chamber. Both blasted and sham mice were given an IP injection (100 mL/20 kg body weight) of buprenorphine (0.003 mg/mL) immediately after the blast or sham blast, respectively.

BRN3A Immunohistochemistry Staining

We followed a well-established protocol to identify RGCs via BRN3A immunohistochemistry, as previously described.[32] After euthanasia, mice were transcardially perfused with 0.01-M PBS followed by 4% paraformaldehyde in 0.01-M PBS. Ipsilateral whole eyes were enucleated and posterior cups were dissected and fixed for 4 hours at 4°C. Posterior cups were incubated overnight in a 0.3% Triton X-100 solution in phosphate-buffered saline (PBST) at 37°C on an agitator. Retinas were dissected and bleached in 3% hydrogen peroxide solution in 1% monobasic sodium phosphate for 3 hours at room temperature. Retinas were permeabilized by freezing the retinas in –80°C for 15 minutes and then blocked in 2% normal donkey serum in PBST overnight on an agitator at 4°C. RGCs were labeled using anti-BRN3A (1:200; sc-8429; Santa Cruz Biotechnology, Dallas, TX, USA) in 2% normal donkey serum, 1% Triton X-100, and 1% dimethyl sulfoxide for two nights on the agitator at

4°C, followed by a secondary antibody (1:200; Alexa Fluor 488 Donkey anti-Goat; Thermo Fisher Scientific, Waltham, MA, USA) for 4 hours at room temperature on an agitator and light protected with aluminum foil covering. Retinas then were counterstained with TO-PRO-3 Iodide (1:1000; Molecular Probes, Eugene, OR, USA) for 20 minutes at room temperature on an agitator, transferred to glass microscopy slides (plus/plus charged), and flat mounted using ProLong Diamond Antifade Mountant (Thermo Fisher Scientific), and coverslipped. Slides were left at room temperature for 24 hours in a dark box, then moved to 4°C until imaging.

BRN3A Imaging Methods

BRN3A-stained, flat-mounted retinas were imaged within 2 weeks of staining by confocal microscopy (Zeiss LSM 710; Carl Zeiss Microscopy, White Plains, NY, USA). Each retina had 12 confocal images (1024 × 1024 pixels, 0.18-mm² image area) taken from non-overlapping fields of three zones of eccentricity (four central, four midcentral, four peripheral), with Z-stacks of three to five images for each image.

Quantification of BRN3A Immunohistochemistry Staining

Images of BRN3A-labeled nuclei were processed in ImageJ (National Institutes of Health, Bethesda, MD, USA), by Z projecting at maximum intensity and compressing the file size. The 12 images were concatenated, and the TO-PRO-3 channel was deleted to create a stack of BRN3A stained nuclei. The Subtract Background tool was used with the rolling ball radius set to 35 pixels, followed by the Smooth tool. Stacks were then converted to binary using Huang dark thresholding. Binary stacks were processed using the Open, Watershed, and Fill Holes functions. The Analyze Particles function was applied to the BRN3A images with particle size set to 20 to 150 µm² and circularity 0 to 1. All quantification was conducted by a masked observer.

Pattern-Evoked Electroretinography

Pattern-evoked electroretinography (PERG) was used to objectively measure the function of RGCs before and after injury. Neutral-position PERG responses were evoked with alternating, reversing, and black and white vertical stimuli using a commercially available instrument (Jorvec Corp., Miami, FL, USA). Mice were anesthetized with a combination of ketamine (50–60 mg/kg, IP), xylazine (8–10 mg/kg, IP), and acepromazine (4–5 mg/kg, IP) and then placed on a heated recording table to maintain body temperature. Commercially available stainless steel subdermal electrodes (Ambu, Ballerup, Denmark) were placed in the snout as a recording electrode, medially at the base of the head as a reference electrode, and at the base of the tail as a ground electrode. Each animal was placed at the same fixed position in front of the monitor to prevent recording variability due to animal placement, with each eye positioned 10 cm from the monitors. The parameters used for recordings were 18° radius visual angle subtended on a full-field pattern, bars 1.5 cm high × 14 cm wide, two reversals per second, 98% contrast, 80 cd/m² average monitor illumination intensity using luminance-matched pattern reversals to exclude outer retinal contributions, and 372 averaged signals with

cutoff filter frequencies of 1 to 30 Hz. Stimuli were delivered under mesopic conditions without dark adaptation to exclude the possible effect of direct photoreceptor-derived evoked responses. A diffuser placed over the pattern on the monitor also did not elicit a measurable evoked potential, further ensuring that the electrical responses were elicited from RGCs. PERG response was evaluated by measuring the amplitude (peak to trough) of the waveform in the eye ipsilateral to the blast wave, as we have described previously.[21,33] Exclusions were made for mice that were breathing too heavily or if their temperature dropped during acquisition, which was monitored constantly throughout the experiment. Changes in each of these parameters can cause interference in signal acquisition. Exclusion criteria were decided on prior to data acquisition for an individual mouse.

Spectral-Domain Optical Coherence Tomography

Optical coherence tomography (OCT) analysis was performed at pre-injury baseline and 5 weeks post-injury using a Spectralis spectral-domain OCT imaging system (Heidelberg Engineering, Heidelberg, Germany) and a 25-dipoter (D) lens for mouse ocular imaging (Heidelberg Engineering). Mice were anesthetized with a combination of ketamine (30 mg/kg, IP) and xylazine (5 mg/kg, IP) and placed on a heating pad to maintain body temperature. Pupils were dilated using a 1% tropicamide solution (Sandoz, Princeton, NJ, USA), and the cornea was moisturized with a balanced saline solution. After the recording, the cornea was moisturized with 0.3% hypromellose (GenTeal Tears, Alcon, Fort Worth, TX, USA). Volume scans (with a pattern size of 20° × 25° and 61 B-lines) were positioned directly over the optic nerve head to quantify the RGC complex thickness, which includes RGC bodies, axons, and dendrites. Scans in the superior retina were analyzed by a masked observer, excluding blood vessels from the RGC complex thickness calculation.

Experimental Design and Statistical Analysis

Supplementary Table S1 provides information regarding all mice utilized in this study. The overall experimental design of the study is depicted in Figure 1. For each analysis, a two-way ANOVA with interaction was conducted, followed by a Tukey's honestly significant difference (HSD) test for all pairwise comparisons. Diagnostics to assess assumptions were performed for each model (QQ plots of residuals, Shapiro–Wilks test of residuals, plots of residuals versus fitted values, and Levene's test, as appropriate).

To investigate whether sex affected each metric, we constructed a WT-only model with factors of sex (male versus female), treatment (blast versus sham), and an interaction between sex and treatment. If no significant sex or sex-by-treatment effect was found in WT mice, then subsequent models were constructed without sex. Next, models were constructed to assess genotype protection from blast injury. For the OCT, the modeled outcome of interest was the change from pretreatment to posttreatment for each mouse. For BRN3A and PERG, the modeled outcome of interest was posttreatment. Additionally, pretreatment models were constructed for OCT and PERG. A natural logarithm transformation, which is commonly used to normalize right-skewed outcomes in regression, was required for the pretreatment PERG in order to meet model assumptions. In each model, factors
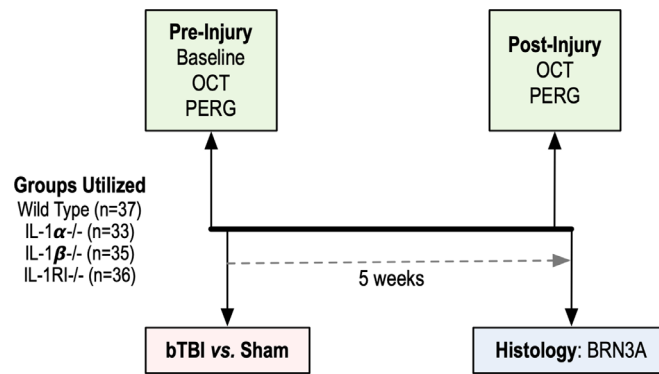
FIGURE 1. Experimental design. OCT and PERG were conducted before injury (bTBI or sham) as a baseline and 5 weeks post-injury, followed by tissue collection for histological analysis to quantitate BRN3A$^+$ retinal ganglion cells. Studies were conducted in both male and female mice.

were genotype (WT versus IL-1$\alpha^{-/-}$ versus IL-1$\beta^{-/-}$ versus IL-1RI$^{-/-}$), treatment (blast versus sham), and interaction between genotype and treatment. *F*-tests were conducted for overall sex, treatment, and interaction effects, and Tukey's HSD was then employed to make inference on all pairwise comparisons. A value of $P < 0.05$ was considered significant. All of the statistical data were presented as mean ± SEM, and analyses were performed in R (R Foundation for Statistical Computing, Vienna, Austria).

RESULTS

Sex Does Not Have an Effect on Visual Outcomes After bTBI

5 weeks after repeated bTBI, we analyzed three different visual outcomes in sham- and blast-exposed mice. First, immunohistochemical labeling of BRN3A (a protein expressed in the majority of RGCs)[34,35] enabled us to determine the total number of RGCs surviving in the retina after injury. Second, OCT measured the *in vivo* thickness of the RGC complex layer, which is made up of RGC cell bodies, axons, and dendrites, providing information about the structural integrity of this retinal layer. Third, PERG evaluated the signaling function of RGCs *in vivo*.

This analysis addressed the unanswered question of whether bTBI has a different effect on male versus female visual systems in WT mice.[34,35] Unsurprisingly, the blast injury significantly affected all three outcomes measured: the number of BRN3A$^+$ RGCs ($P < 0.0001$; $F = 66.12$; $df = 1, 41$) (Fig. 2A), the thickness of the RGC complex layer ($P < 0.0001$; $F = 78.57$; $df = 1, 62$) (Fig. 2B), and RGC function ($P < 0.0001$; $F = 66.59$; $df = 1, 70$) (Fig. 2C). Moreover, sex did not have an effect on any outcomes for WT mice as determined by two-way ANOVA with Tukey's HSD posttest (Fig. 2; Supplementary Tables S2–S4 contain *P* values for group comparisons). Specifically, both sexes contained similar numbers of BRN3A$^+$ cells ($P = 0.1089$; $F = 2.69$; $df = 1, 41$) (Fig. 2A), and exposure to sham or blast forces caused similar responses in BRN3A$^+$ RGCs in WT mice regardless of sex ($P = 0.9594$ and $P = 0.2606$, respectively). Similarly, sex had no effect on the blast-induced thinning of the RGC complex layer ($P = 0.8977$; $F = 0.017$; $df = 1, 62$) (Fig. 2B), with a non-significant difference between male and female groups in WT sham and WT blast mice ($P = 0.9986$ and $P = 0.8768$, respectively). Sex did not influence blast-

induced changes in PERG amplitude ($P = 0.2558$; $F = 1.31$; $df = 1, 70$) (Fig. 2C), with a non-significant difference between male and female groups in WT sham and WT blast mice ($P = 0.9878$ and $P = 0.9182$, respectively). Finally, there was no significant sex by treatment effect on any outcome: BRN3A$^+$ RGCs ($P = 0.4096$; $F = 0.69$; $df = 1, 41$) (Fig. 2A), change in RGC complex layer thickness via OCT analysis ($P = 0.52$; $F = 0.42$; $df = 1, 62$) (Fig. 2B), and RGC function via PERG analysis ($P = 0.8618$; $F = 0.031$; $df = 1, 70$) (Fig. 2C). Because we determined that the sex of the mice does not affect the visual outcomes we were measuring, male and female mice were pooled for the rest of our analyses; WT groups in Figures 3 through 5 are pooled male and female groups from Figure 2.

RGC Quantification Via BRN3A Immunohistochemistry

BRN3A immunohistochemistry allowed for a quantitative analysis of the number of RGCs in the retinas of WT, IL-1$\alpha^{-/-}$, IL-1$\beta^{-/-}$, and IL-1RI$^{-/-}$ mice, so we determined the density of RGCs 5 weeks after exposure to either sham or blast injury (Fig. 3; Supplementary Table S5). For IL-1$\beta^{-/-}$ knockout (KO) mice, blast and sham groups had similar numbers of RGCs ($P = 0.2985$), suggesting that in the absence of IL-1β RGCs are protected from blast injury. In contrast, IL-1$\alpha^{-/-}$ and IL-1RI$^{-/-}$ mice appeared to be more injured by the blasts, as the WT, IL-1$\alpha^{-/-}$, and IL-1RI$^{-/-}$ blast groups had significantly fewer RGCs than the sham groups ($P < 0.0001$, $P = 0.0008$, $P < 0.0001$, respectively). Still, the IL-1$\alpha^{-/-}$ and IL-1$\beta^{-/-}$ mice appeared to have partial protection, as the WT mice had significantly fewer BRN3A$^+$ RGCs than the KO counterparts ($P = 0.0080$ and $P < 0.0001$, respectively). In addition, WT blast mice had the largest percent decrease in BRN3A$^+$ RGCs (39.96%); however, for IL-1$\alpha^{-/-}$, IL-1$\beta^{-/-}$, and IL-1RI$^{-/-}$ mice, the percent changes between sham and blast groups were –21.97%, –11.10%, and –29.30%, respectively (Table 1), further suggesting that in the absence of these IL-1 proteins the RGCs were partially protected.

Blast-Induced RGC Injury After Repeated bTBI

Before blast exposure, the baseline thickness of the RGC complex layer of ipsilateral eyes was similar for sham and blast mice within the WT, IL-1$\alpha^{-/-}$, IL-1$\beta^{-/-}$, and IL-

A. RGC COUNT

B. OCT

C. PERG
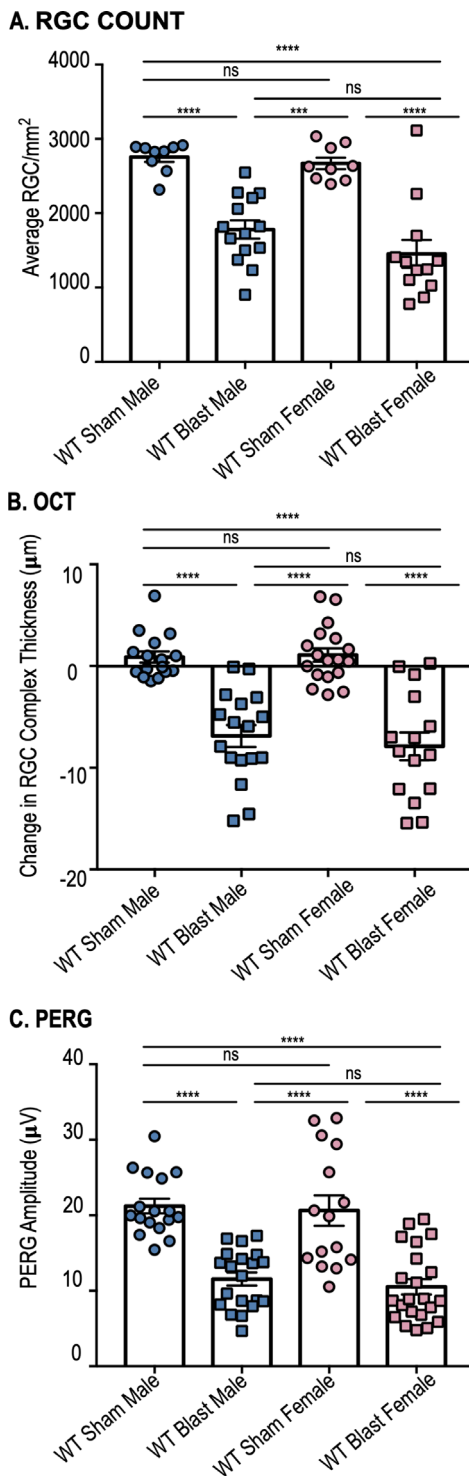
FIGURE 2. Sex did not have an effect on visual outcomes after repeated blast exposure in male and female WT mice at 5 weeks post-injury. There was no sex effect detected between sham groups or blast groups when comparing (**A**) number of BRN3A+ RGCs ($P = 0.1089$; $n = 9$-14), (**B**) change in RGC complex layer thickness via OCT analysis ($P = 0.8977$; $n = 15$–18), or (**C**) RGC function via PERG analysis ($P = 0.2558$; $n = 15$–22). Blast treatment was determined to have a significant effect on all three outcomes ($P < 0.0001$). P values for group comparisons can be found in Supplementary Tables S2 to S4. All data are from ipsilateral retinas and are expressed as mean ± SEM; significance was determined by two-way ANOVA with interaction effect followed by Tukey's HSD posttest of all pairwise comparisons of means.

TABLE 1. Mean ± SEM and Percent Difference from Sham of Total Number of BRN3A-Positive RGCs for Each Group

Group	Mean ± SEM	Percent Change from Sham
WT sham	2713 ± 51	
WT blast	1629 ± 112	−39.96%
IL-1$\alpha^{-/-}$ sham	2731 ± 95	
IL-1$\alpha^{-/-}$ blast	2131 ± 123	−21.97%
IL-1$\beta^{-/-}$ sham	3037 ± 106	
IL-1$\beta^{-/-}$ blast	2700 ± 104	−11.10%
IL-1RI$^{-/-}$ sham	2597 ± 55	
IL-1RI$^{-/-}$ blast	1836 ± 115	−29.30%

1RI$^{-/-}$ groups ($P = 0.9999$, $P = 1.0000$, $P = 1.0000$, and $P = 1.0000$, respectively) (Fig. 4C; Supplementary Table S6). At 5 weeks post-blast injury, all genotypes showed RGC complex layers that were thinner than their sham counterparts (WT, IL-1$\alpha^{-/-}$, IL-1$\beta^{-/-}$, and IL-1RI$^{-/-}$ at $P < 0.0001$, $P < 0.0001$, $P = 0.0107$, and $P < 0.0001$, respectively) (Fig. 4D; Supplementary Table S7). However, when comparing blast-exposed WT to blast-exposed IL-1$\alpha^{-/-}$ or IL-1$\beta^{-/-}$ mice, genetic KO mice had significantly thicker RGC complex layers than WT ($P = 0.0410$ and $P < 0.0011$, respectively) (Supplementary Table S7). This suggests that IL-1$\alpha^{-/-}$ and IL-1$\beta^{-/-}$ mice are partially protected from RGC complex layer loss, mirroring the trend we detected by BRN3A$^+$ RGC quantification (Fig. 3B). Also similar to the findings with the RGC quantification, WT mice exposed to blast showed the most thinning in their RGC complex layer (–11.24%), whereas, compared to sham treatment, blast-exposed IL-1$\alpha^{-/-}$, IL-1$\beta^{-/-}$, and IL-1RI$^{-/-}$ mice showed less RGC thinning (i.e., –6.71%, –4.47%, and –7.43%, respectively) (Table 2).

The functional signaling capacity of RGCs is reflected by PERG amplitudes. In our mice, the pre-injury baseline, peak-to-trough amplitudes for the ipsilateral eyes were not significantly different between sham and blast mice within the WT, IL-1$\alpha^{-/-}$, IL-1$\beta^{-/-}$, and IL-1RI$^{-/-}$ groups ($P = 0.6305$, $P = 1.0000$, $P = 0.9778$, and $P = 0.9997$, respectively) (Fig. 5A; Supplementary Table S8). However, 5 weeks post-injury, the blast-treated mice in all groups showed a significant decrease in their PERG amplitudes when compared to sham, indicative of RGC signaling deficits ($P < 0.0001$, $P = 0.0239$, $P = 0.0024$, and $P = 0.0089$, respectively) (Fig. 5B; Supplementary Table S9). Interestingly, when comparing the WT blast group to the KO blast groups, the IL-1$\alpha^{-/-}$ and IL-1R$^{-/-}$ mice had significantly higher PERG amplitudes ($P < 0.0001$ and $P = 0.0037$, respectively), whereas the IL-1$\beta^{-/-}$ blast group was not significantly different ($P = 0.0548$), suggesting that removal of the IL-1α and IL-1RI molecules could confer some protection for RGC signaling within the retina after blast injury. Among the groups analyzed, WT mice exposed to bTBI had the largest decrease in number of RGCs and had the thinnest RGC complex layer as compared to their sham counterparts; similarly, they showed the most dampened RGC signaling, at –47.42%. Comparatively, RGC signaling in the IL-1$\alpha^{-/-}$, IL-1$\beta^{-/-}$, and IL-1RI$^{-/-}$ blast groups was less affected compared to sham cohorts, at –20.06%, –26.55%, and –24.25%, respectively (Table 3).

DISCUSSION

The majority of previous studies in the literature were conducted with male animals, but sex might affect neuroin-
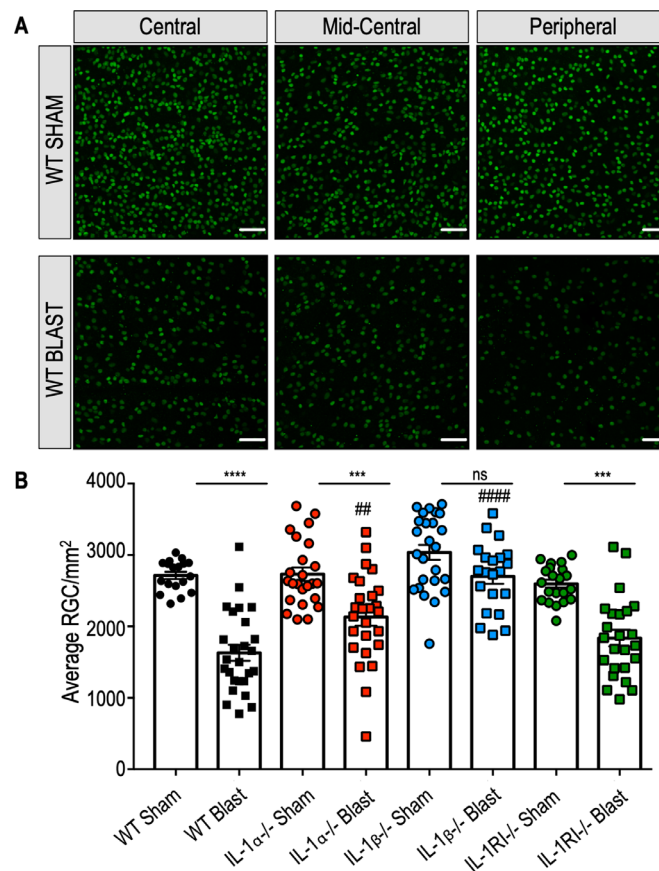
FIGURE 3. Retinal ganglion cell quantification 5 weeks after repeated blast exposure. BRN3A^{+} RGCs in retinal whole-mounts exposed to sham or blast injury. (**A**) Representative images of WT retinas taken in central, mid-central, and peripheral locations. (**B**) Retinas from WT sham animals had significantly more RGCs when compared to WT blast animals ($P < 0.0001$). Within genotypes, the IL-1$\alpha^{-/-}$ and IL-1RI$^{-/-}$ blast mice had significantly fewer RGCs than the sham counterparts ($P = 0.0008$ and $P < 0.0001$, respectively). However, the IL-1$\beta^{-/-}$ blast group was not significantly different from the sham group, suggesting partial protection from RGC loss ($P = 0.2985$). When compared to the WT blast group, the IL-1$\alpha^{-/-}$ and IL-1$\beta^{-/-}$ blast groups had significantly more BRN3A^{+} RGCs ($P = 0.0080$ and $P < 0.0001$, respectively), suggesting protection from blast injury. Significance was determined by two-way ANOVA with interaction effect followed by Tukey's HSD posttest testing all pairwise comparisons of means. * indicates significant difference within genotypes; # indicates significant difference compared to the WT blast group. Data are expressed as mean ± SEM; $n = 18$–26. Original magnification, 25×; en face view with the RGC layer facing up. *Scale bar*: 100 µm.

TABLE 2. Mean ± SEM for the Change in Measurements from Baseline, Pre-Injury Measurements, and Post-Injury Measurements for RGC Complex Layer Thickness

	Mean ± SEM (µm)			
	Change from Baseline	**Pre-Injury**	**Post-Injury**	**Percent Change from Sham**
WT sham	1.00 ± 0.43	71.34 ± 0.36	72.34 ± 0.32	
WT blast	−7.35 ± 0.85	71.56 ± 0.39	64.21 ± 0.96	−11.24%
IL-1$\alpha^{-/-}$ sham	0.52 ± 0.33	74.69 ± 0.45	75.21 ± 0.43	
IL-1$\alpha^{-/-}$ blast	−4.54 ± 0.97	74.7 ± 0.46	70.16 ± 0.92	−6.71%
IL-1$\beta^{-/-}$ sham	−0.23 ± 0.42	74.28 ± 0.42	74.04 ± 0.34	
IL-1$\beta^{-/-}$ blast	−3.50 ± 0.83	74.23 ± 0.35	70.73 ± 0.96	−4.47%
IL-1RI$^{-/-}$ sham	0.06 ± 0.36	73.55 ± 0.37	73.6 ± 0.31	
IL-1RI$^{-/-}$ blast	−5.51 ± 0.63	73.64 ± 0.43	68.13 ± 0.59	−7.43%

Percent difference from sham was calculated from post-injury values.

flammatory injury and repair mechanisms after TBI. Although more recent studies have begun using both male and female mice, some studies report that females fare better than males, and vice versa, while still others have found no difference between the sexes or had unclear results.[25]

CNS anatomy, cellular pathways, and drug responses can be affected by sex,[36–38] but the specific parameters being analyzed could additionally produce different conclusions, depending on the effect of sex hormones. Indeed, sex-specific responses to the injury, the reparative processes that

TABLE 3. Mean ± SEM for Pre-Injury Baseline and Post-Injury Measurements of PERG Amplitudes Reflective of RGC Signaling

| | Mean ± SEM (µV) | | |
	Pre-Injury	Post-Injury	Percent Change from Sham
WT sham	23.03 ± 0.79	20.94 ± 1.06	
WT blast	21.14 ± 0.61	11.01 ± 0.67	−47.42%
IL-1$\alpha^{-/-}$ sham	25.49 ± 0.96	24.33 ± 1.11	
IL-1$\alpha^{-/-}$ blast	25.42 ± 0.95	19.45 ± 1.2	−20.06%
IL-1$\beta^{-/-}$ sham	20.22 ± 0.79	20.53 ± 0.90	
IL-1$\beta^{-/-}$ blast	21.08 ± 0.75	15.08 ± 1.09	−26.55%
IL-1RI$^{-/-}$ sham	24.29 ± 0.79	21.32 ± 0.93	
IL-1RI$^{-/-}$ blast	23.74 ± 0.74	16.15 ± 1.00	−24.25%

Percent difference from sham was calculated from post-injury values.

occur later, and responses to therapeutic interventions could result in distinctly different patterns of neuroprotection or neurodegeneration.

Here, we found that sex had no effect on visual outcomes after bTBI. WT sham versus blast changes were similar in male and female cohorts. This lack of a sex-specific difference in injury response is an important and novel finding that can direct future study design. Nevertheless, this conclusion can only be made for the specific parameters analyzed in this study, and the biologic variable of sex still has to be explored further to determine its overall role in bTBI pathogenesis. Of note, the estrus phase of the female mice was not monitored throughout the course of the experiments, which means that cyclic hormonal changes could be a potential limitation of the study design.

Generally, constitutively deleting the genes encoding IL-1α, IL-1β, or IL-1RI did not fully rescue the RGC damage seen in blast-injured mice within genotypes. The exception was with the deletion of IL-1β, which increased the number of surviving RGC cells after blast (Fig. 3B). This is in contrast to the effect of IL-1RI pharmacological block with anakinra, which prevents both IL-1α and IL-1β cytokine signaling and protects mice from blast injury.[19] Nevertheless, the percent change between sham and blast groups in the number of surviving RGCs, RGC complex layer thickness, and RGC signaling was smaller for all three KO groups when compared to WT, suggesting that partial protection might be conferred by removal of these IL-1 pathway components and that these molecules may play a role in post-bTBI injury pathogenesis (Tables 1–3). When comparing the blast cohorts, some KOs demonstrated significantly less damage than the WT mice, again suggesting that the loss of these molecules may provide partial protection from retinal injury after bTBI. When compared to the WT blast group, the IL-1$\alpha^{-/-}$ and IL-1$\beta^{-/-}$ blast groups had significantly more surviving RGCs (Fig. 3B) and a significantly thicker RGC complex layer (Fig. 4D), suggesting enhanced structural preservation of this retinal layer. Interestingly, compared to the WT blast group, the IL-1$\alpha^{-/-}$ and IL-1RI$^{-/-}$ blast groups had significantly preserved RGC signaling (Fig. 5B). Although this observation might suggest that impaired IL-1 signaling tends to partially protect from bTBI damage, these data should be interpreted with caution because, prior to injury, the blast cohorts showed significant differences in OCT and PERG measurements, which could be a confounding factor when making comparisons across genotypes (Supplementary Tables S6 and S8).

We had hypothesized that genetically impairing IL-1RI signaling would protect mice similarly to the pharmacologic

blockade of IL-1RI via anakinra, but this was not the finding of this study. The lack of a strong rescue with the genetic deletion of these genes could have several explanations. It is possible the constitutive knockouts may not rescue visual outcomes because they are compensated for during development, or perhaps deletion from birth differs from acute blockade. Because inflammation is a complex and redundant process wherein many molecules provide overlapping functions to create an equilibrium between destructive and reparative processes, it is possible that other inflammatory modulators might have been upregulated early on to offset impaired IL-1 signaling. Innate immune signaling through other IL-1 family molecules (IL-18, IL-33, IL-36, IL-37, and IL-38) or through other pathways such as TNFα or IL-6 could be altered in these mice. Alternatively, as inflammation is known to have a dichotomous effect, it is possible that IL-1 pathway molecules are also a part of an important reparative process specific to bTBI, and complete blockade could actually hinder retinal recovery after blast injury.

Finally, the previously published effects of treatment with anakinra may be due (or due in part) to off-target effects unrelated to the IL-1RI, a potential problem for any pharmacologic intervention. To address these questions, future studies will include the use of inducible IL-1RI knockout lines, allowing us to delete IL-1 pathway components after development is completed. If the mechanism of visual protection truly functions through IL-1RI but is compensated for during development in constitutive IL-1RI KOs, then temporally blocking IL1RI around the time of bTBI might rescue visual deficits seen after blast. In addition, potential off-target effects of anakinra will have to be explored in order to elucidate this mechanism to develop new treatments for TBI-mediated visual loss.

As with all animal models, it is important to note that there are several limitations of this study that have not been mentioned previously. This analysis focused solely on retinal consequences after blast injury, as RGC dysfunction is one of the most frequently reported symptoms. Damage to the optic nerve or other higher visual pathways was not evaluated, but future analysis of this tissue could provide vital mechanistic information. Additionally, although RGC survival, RGC complex layer integrity, and RGC function were evaluated, no behavioral testing reflective of overall visual acuity and function was carried out. The RGC complex layer was the only retinal layer evaluated via OCT when other groups have looked at changes in different cell types after ocular injury. Finally, although the repetitive bTBI model is reflective of human injury, the mice are anesthetized prior to each
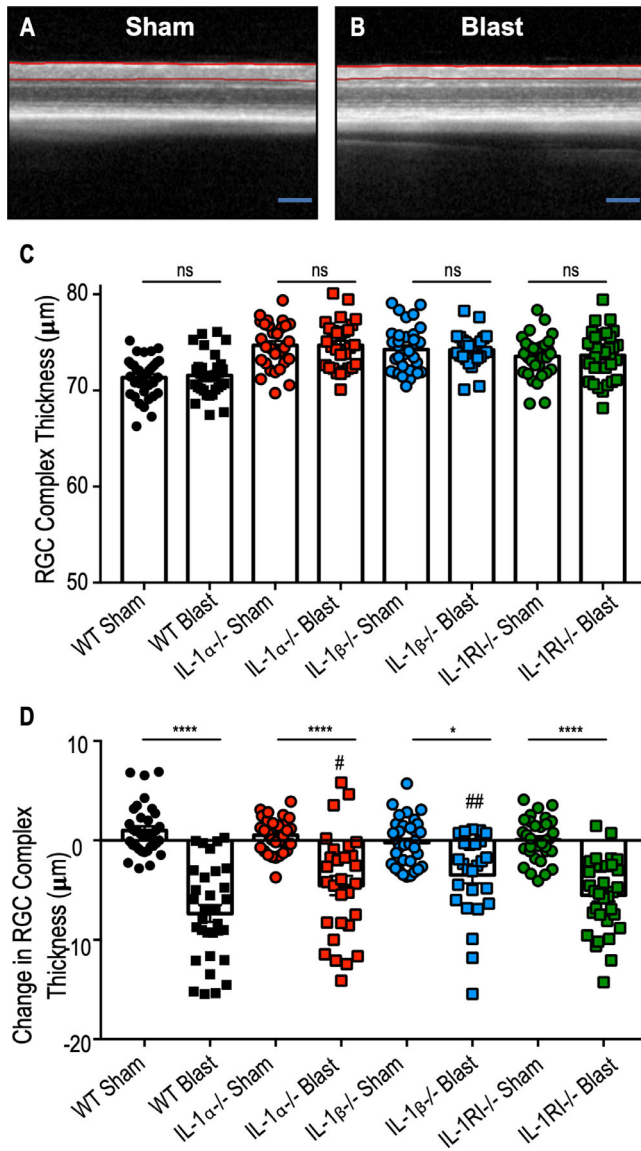
FIGURE 4. The RGC complex layer was thinner after repeated blast exposure. (**A**, **B**) Representative OCT images of sham (**A**) and blast (**B**) groups. (**C**) Baseline measurements of the thickness of the RGC complex layer were taken prior to injury, showing no significant differences between the blast and sham groups for all genotypes. (**D**) At 5 weeks post-injury, the blast-treated mice had a significantly thinner RGC complex layer compared to baseline measurements when compared to the sham counterparts in the WT, IL-$1\alpha^{-/-}$, IL-$1\beta^{-/-}$, and IL-1RI$^{-/-}$ genotypes ($P < 0.0001$, $P < 0.0001$, $P = 0.0107$, and $P < 0.0001$, respectively). When comparing the WT blast group to the IL-$1\alpha^{-/-}$ and IL-$1\beta^{-/-}$ blast groups, the RGC complex layer was significantly thicker in the null mice ($P = 0.0410$ and $P < 0.0011$, respectively), suggesting partial protection from RGC complex layer loss. All data are from ipsilateral retinas. Significance was determined by two-way ANOVA with interaction effect followed by Tukey's HSD posttest testing all pairwise comparisons of means. * indicates significant difference within genotypes; # indicates significant difference compared to WT blast. Data are expressed as mean ± SEM; $n = 26$–34. *Scale bar*: 200 μm.
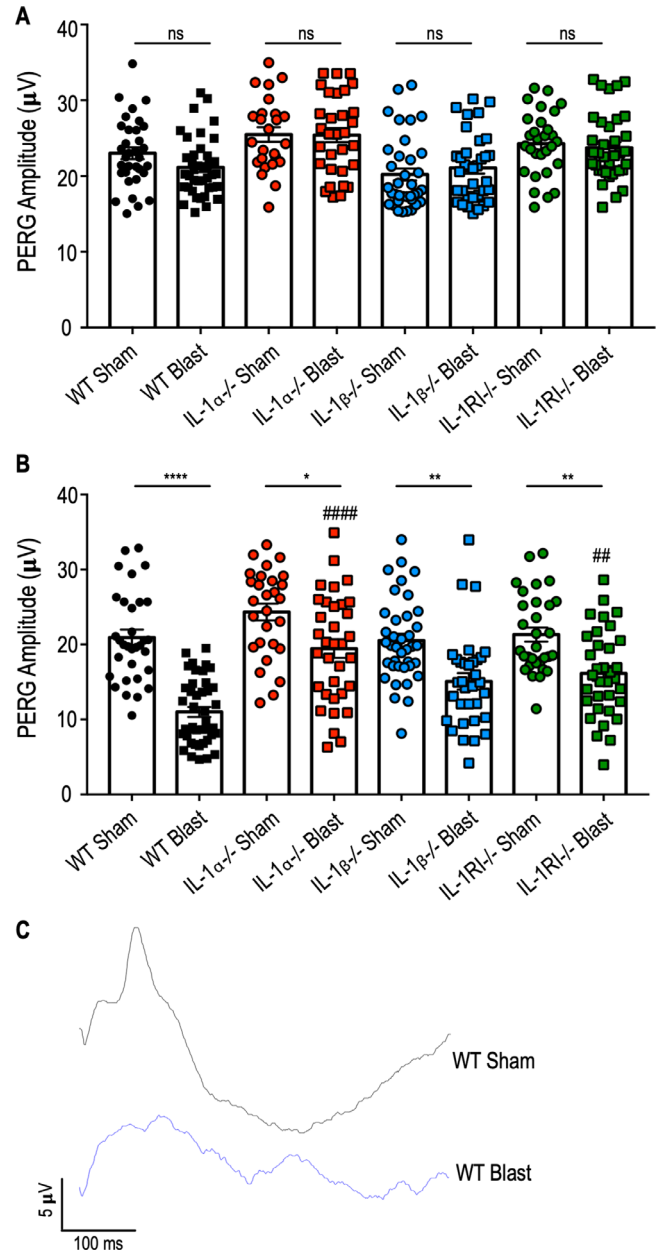
FIGURE 5. RGC dysfunction was observed after repeated blast. (**A**) Baseline measurements of RGC signaling were taken before blast injury using PERG, with no significant differences between blast and sham mice within each genotype. (**B**) At 5 weeks post-injury, PERG analysis revealed blast versus sham deficits in the WT, IL-$1\alpha^{-/-}$, IL-$1\beta^{-/-}$, and IL-1RI$^{-/-}$ groups ($P < 0.0001$, $P = 0.0239$, $P = 0.0024$, and $P < 0.0089$, respectively). When compared to the WT blast group, the IL-$1\alpha^{-/-}$ and IL-1RI$^{-/-}$ counterparts had significantly higher PERG amplitudes ($P < 0.0001$ and $P = 0.0037$, respectively), suggesting partial protection from RGC signaling damage after blast injury. (**C**) Representative WT sham and blast PERG waveforms are shown in *black* and *blue*, respectively. All PERG recordings are of ipsilateral eyes and were measured in the neutral position. Significance was determined by two-way ANOVA with interaction effect followed by Tukey's HSD posttest testing all pairwise comparisons of means. * indicates significant difference within genotypes; # indicates significant difference compared to WT blast. Data are expressed as means ± SEM; $n = 28$–42.

blast, making the effects of repetitive anesthesia exposure a possible confounding variable. In our study, both the sham and blast mice were given the identical dosages in order to ensure that their conditions were as similar as possible aside from the blast itself.

The findings of this study indicate that sex does not affect the RGC outcomes assessed after murine bTBI. The included genetic studies suggest that deletion of IL-1 pathway components confers some protection, but global deletion from birth did not result in a complete rescue. Further studies elucidating the role of IL-1 in the eye after bTBI are necessary to understand this complex and heterogeneous injury.

Disclosure: **L.P. Evans**, None; **N. Boehme**, None; **S. Wu**, None; **E.L. Burghardt**, None; **A. Akurathi**, None; **B.P. Todd**, None; **E.A. Newell**, None; **P.J. Ferguson**, None; **V.B. Mahajan**, None; **L.M. Dutca**, None; **M.M. Harper**, None; **A.G. Bassuk**, None

References

1. Hoge CW, McGurk D, Thomas JL, Cox AL, Engel CC, Castro CA. Mild traumatic brain injury in U.S. soldiers returning from Iraq. *N Engl J Med*. 2008;358(20):453–463.

2. Lew HL, Poole JH, Guillory SB, Salerno RM, Leskin G, Sigford B. Persistent problems after traumatic brain injury: the need for long-term follow-up and coordinated care. *J Rehabil Res Dev*. 2006;43(2):vii–x.

3. Armstrong RA. Visual problems associated with traumatic brain injury. *Clin Exp Optom*. 2018;101(6):716–726.

4. Das M, Tang X, Mohapatra SS, Mohapatra S. Vision impairment after traumatic brain injury: present knowledge and future directions. *Rev Neurosci*. 2019;30(3):305–315.

5. Kapoor N, Ciuffreda KJ. Vision disturbances following traumatic brain injury. *Curr Treat Options Neurol*. 2002;4(4):271–280.

6. Suchoff IB, Kapoor N, Ciuffreda KJ, Rutner D, Han E, Craig S. The frequency of occurrence, types, and characteristics of visual field defects in acquired brain injury: a retrospective analysis. *Optometry*. 2008;79(5):259–265.

7. Defense and Veterans Brain Injury Center. DoD worldwide numbers for TBI. Available at: https://dvbic.dcoe.mil/dod-worldwide-numbers-tbi . Accessed June 17, 2020.

8. Cho RI, Bakken HE, Reynolds ME, Schlifka BA, Powers DB. Concomitant cranial and ocular combat injuries during Operation Iraqi Freedom. *J Trauma*. 2009;67(3):516–520; discussion 519–520.

9. Cockerham GC, Goodrich GL, Weichel ED, et al. Eye and visual function in traumatic brain injury. *J Rehabil Res Dev*. 2009;46(6):811–818.

10. Cockerham GC, Rice TA, Hewes EH, et al. Closed-eye ocular injuries in the Iraq and Afghanistan wars. *N Engl J Med*. 2011;364(22):2172–2173.

11. Dougherty AL, MacGregor AJ, Han PP, Heltemes KJ, Galarneau MR. Visual dysfunction following blast-related traumatic brain injury from the battlefield. *Brain Inj*. 2011;25(1):8–13.

12. Simon DW, McGeachy MJ, Bayir H, Clark RSB, Loane DJ, Kochanek PM. The far-reaching scope of neuroinflammation after traumatic brain injury. *Nat Rev Neurol*. 2017;13(3):171–191.

13. Hutchinson PJ, O'Connell MT, Rothwell NJ, et al. Inflammation in human brain injury: intracerebral concentrations of IL-1alpha, IL-1beta, and their endogenous inhibitor IL-1ra. *J Neurotrauma*. 2007;24(10):1545–1557.

14. Allan SM, Tyrrell PJ, Rothwell NJ. Interleukin-1 and neuronal injury. *Nat Rev Immunol*. 2005;5(8):629–640.

15. Utagawa A, Truettner JS, Dietrich WD, Bramlett HM. Systemic inflammation exacerbates behavioral and histopathological consequences of isolated traumatic brain injury in rats. *Exp Neurol*. 2008;211(1):283–291.

16. London A, Benhar I, Schwartz M. The retina as a window to the brain-from eye research to CNS disorders. *Nat Rev Neurol*. 2013;9(1):44–53.

17. Hue CD, Cho FS, Cao S, et al. Time course and size of blood-brain barrier opening in a mouse model of blast-induced traumatic brain injury. *J Neurotrauma*. 2016;33(13):1202–1211.

18. Evans LP, Newell EA, Mahajan M, et al. Acute vitreoretinal trauma and inflammation after traumatic brain injury in mice. *Ann Clin Transl Neurol*. 2018;5(3):240–251.

19. Evans LP, Woll AW, Wu S, et al. 2020 modulation of posttraumatic immune response using the IL-1 receptor antagonist anakinra for improved visual outcomes. *J Neurotrauma*. 2020;37(12):1463–1480.

20. Struebing FL, King R, Li Y, et al. Transcriptional changes in the mouse retina after ocular blast injury: a role for the immune system. *J Neurotrauma*. 2018;35(1):118–129.

21. Mohan K, Kecova H, Hernandez-Merino E, Kardon RH, Harper MM. Retinal ganglion cell damage in an experimental rodent model of blast-mediated traumatic brain injury. *Invest Ophthalmol Vis Sci*. 2013;54(5):3440–3450.

22. Bricker-Anthony C, Hines-Beard J, Rex TS. Eye-directed overpressure airwave-induced trauma causes lasting damage to the anterior and posterior globe: a model for testing cell-based therapies. *J Ocul Pharmacol Ther*. 2016;32(5):286–295.

23. Dutca LM, Stasheff SF, Hedberg-Buenz A, et al. Early detection of subclinical visual damage after blast-mediated TBI enables prevention of chronic visual deficit by treatment with P7C3-S243. *Invest Ophthalmol Vis Sci*. 2014;55(12):8330–8341.

24. Yin TC, Voorhees JR, Genova RM, et al. Acute axonal degeneration drives development of cognitive, motor, and visual deficits after blast-mediated traumatic brain injury in mice. *eNeuro*. 2016;3(5):ENEURO.0220–16.2016.

25. Gupte R, Brooks W, Vukas R, Pierce J, Harris J. Sex differences in traumatic brain injury: what we know and what we should know. *J Neurotrauma*. 2019;36(22):3063–3091.

26. Glaccum MB, Stocking KL, Charrier K, et al. Phenotypic and functional characterization of mice that lack the type I receptor for IL-1. *J Immunol*. 1997;159(7):3364–3371.

27. Horai R, Asano M, Sudo K, et al. Production of mice deficient in genes for interleukin (IL)-1α, IL-1β, IL-1α/β, and IL-1 receptor antagonist shows that IL-1β is crucial in turpentine-induced fever development and glucocorticoid secretion. *J Exp Med*. 1998;187(9):1463–1475.

28. Vest V, Bernardo-Colon A, Watkins D, Kim B, Rex TS. Rapid repeat exposure to subthreshold trauma causes synergistic

axonal damage and functional deficits in the visual pathway in a mouse model. *J Neurotrauma*. 2019;36(10):1646–1654.

29. Meabon JS, Huber BR, Cross DJ, et al. Repetitive blast exposure in mice and combat veterans causes persistent cerebellar dysfunction. *Sci Transl Med*. 2016;8(321):321ra326.

30. Peskind ER, Petrie EC, Cross DJ, et al. Cerebrocerebellar hypometabolism associated with repetitive blast exposure mild traumatic brain injury in 12 Iraq war Veterans with persistent post-concussive symptoms. *NeuroImage*. 2011;54(suppl. 1):S76–S82.

31. Petrie EC, Cross DJ, Yarnykh VL, et al. Neuroimaging, behavioral, and psychological sequelae of repetitive combined blast/impact mild traumatic brain injury in Iraq and Afghanistan war veterans. *J Neurotrauma*. 2014;31(5):425–436.

32. Harper MM, Woll AW, Evans LP, et al. Blast preconditioning protects retinal ganglion cells and reveals targets for prevention of neurodegeneration following blast-mediated traumatic brain injury. *Invest Ophthalmol Vis Sci*. 2019;60(13):4159–4170.

33. Mohan K, Harper MM, Kecova H, et al. Characterization of structure and function of the mouse retina using pattern electroretinography, pupil light reflex, and optical coherence tomography. *Vet Ophthalmol*. 2012;15(suppl. 2):94–104.

34. Mead B, Thompson A, Scheven BA, Logan A, Berry M, Leadbeater W. Comparative evaluation of methods for estimating retinal ganglion cell loss in retinal sections and wholemounts. *PLoS One*. 2014;9(10):e110612.

35. Rodriguez AR, de Sevilla Muller LP, Brecha NC. The RNA binding protein RBPMS is a selective marker of ganglion cells in the mammalian retina. *J Comp Neurol*. 2014;522(6):1411–1443.

36. McCarthy MM, Pickett LA, VanRyzin JW, Kight KE. Surprising origins of sex differences in the brain. *Horm Behav*. 2015;76:3–10.

37. Soldin OP, Mattison DR. Sex differences in pharmacokinetics and pharmacodynamics. *Clin Pharmacokinet*. 2009;48(3):143–157.

38. Wagner AK, Kline AE, Ren D, et al. Gender associations with chronic methylphenidate treatment and behavioral performance following experimental traumatic brain injury. *Behav Brain Res*. 2007;181(2):200–209.